

# Role of Electronic Correlations in the Fermi Surface Formation of $\text{Na}_x\text{CoO}_2$ <sup>¶</sup>

A. Shorikov<sup>a</sup>, M. M. Korshunov<sup>b-d</sup>, and V. I. Anisimov<sup>a</sup>

<sup>a</sup> Institute of Metal Physics Ural Division, Russian Academy of Sciences,  
Yekaterinburg GSP-170, 620219 Russia

<sup>b</sup> Kirensky Institute of Physics, Siberian Branch, Russian Academy of Sciences,  
Krasnoyarsk, 660036 Russia

<sup>c</sup> Max-Planck-Institut für Physik komplexer Systeme, D-01187 Dresden, Germany

<sup>d</sup> Department of Physics, University of Florida, Gainesville, Florida 32611, USA

e-mail: korshunov@phys.ufl.edu

Received December 6, 2010

Band structure of metallic sodium cobaltate  $\text{Na}_x\text{CoO}_2$  ( $x = 0.33, 0.48, 0.61, 0.72$ ) has been investigated by local density approximation + Hubbard  $U$  (LDA+ $U$ ) method and within Gutzwiller approximation for the Co- $t_{2g}$  manifold. Correlation effects being taken into account results in suppression of the  $e_g'$  hole pockets at the Fermi surface in agreement with recent angle-resolved photoemission spectroscopy (ARPES) experiments. In the Gutzwiller approximation the bilayer splitting is significantly reduced due to the correlation effects. The formation of high spin (HS) state in Co  $d$ -shell was shown to be very improbable.

DOI: 10.1134/S0021364011020123

## 1. INTRODUCTION

Puzzling properties of sodium cobaltate  $\text{Na}_x\text{CoO}_2$  are the topic of many recent theoretical and experimental investigations [1]. This material holds much promise for thermoelectronics due to its large thermopower [2] together with the relatively low resistivity [3]. The discovery of superconductivity with  $T_c$  about 5 K in  $\text{Na}_{0.33}\text{CoO}_2 \cdot 1.3\text{H}_2\text{O}$  [3] revived the interest in lamellar sodium cobaltates. Moreover, the charge and magnetic long range orders on the frustrated triangular lattice of cobaltate is of the fundamental interest. The band theory predict the complicated Fermi surface (FS) with one large hole pocket around the  $\Gamma = (0, 0, 0)$  point and six small pockets near the  $K = \left(0, \frac{4\pi}{3}, 0\right)$

points of the hexagonal Brillouin zone at least for  $x < 0.5$  [4, 5]. However, intensive investigations by several ARPES groups reveal absence of six small pockets in both  $\text{Na}_x\text{CoO}_2 \cdot y\text{H}_2\text{O}$  and in its parent compound  $\text{Na}_x\text{CoO}_2$  [6–10].

The disagreement between ARPES spectra and ab initio calculated band structure points to the importance of the electronic correlations in these oxides. Other evidences for the correlated behavior come from the data on an anomalous Hall effect and a drop of the thermopower in holistic magnetic field [11].

The six hole pockets are absent in the L(S)DA+ $U$  calculations [12, 13]. However, in this approach, the insulating gap is formed by a splitting of the local single-electron states due to spin-polarization, resulting in a spin polarized Fermi surface with an area twice as large as that observed through ARPES. Moreover, the long range ferromagnetic order has been set by hand because of limitation of LDA+ $U$ . The predicted large local magnetic moments as well as the splitting of bands can be considered as artifacts of the L(S)DA+ $U$  method.

Although LDA+ $U$  method is usually applied to describe insulators [14], there are some achievement in investigation of metals and metallic compounds [15, 16]. To analyze the effect of electronic correlations on the Fermi surface formation in sodium cobaltate we employ non-magnetic LDA+ $U$  method. Then, we use a Gutzwiller approximation to display the effect of correlations on the bilayer splitting and compare it with LDA+ $U$  results.

Co  $d$ -level splits by crystal field of oxygen octahedron in lower  $t_{2g}$  and higher  $e_g$  bands. The deficiency of Na in  $\text{Na}_x\text{CoO}_2$  introduces additional holes in the system. Cobalt, having  $d^6$  configuration and filled  $t_{2g}$  shell in parent  $\text{NaCoO}_2$ , is nonmagnetic. But in non-stoichiometric compound part of Co ions become magnetic with local moment about  $1\mu_B$ . This value is provided by  $d^5$  configuration and one hole in  $t_{2g}$  shell. However, the experiments revealed the magnetic susceptibility at room temperature that is much higher

<sup>¶</sup>The article is published in the original.

than it was expected for dilute magnetic impurity in non-magnetic solvent. Explanation of this anomaly was suggested in [17] as transition from low-spin (LS) state with six  $d$ -electrons on  $t_{2g}$  shell to high-spin (HS) state with five  $d$ -electrons on  $t_{2g}$  shell and one electron on  $e_g$ . The possibility of such transition will be discussed below.

## 2. LDA+ $U$ RESULTS

$\text{Na}_{0.61}\text{CoO}_2$  crystallize in the hexagonal unit cell ( $P\bar{6}_3/mmc$  space group) with  $a = 2.83176(3)$  Å and  $c = 10.8431(2)$  Å at 12 K [18]. Displacement of Na atoms from their ideal sites  $2d$  ( $1/3, 2/3, 3/4$ ) on about 0.2 Å are observed in non-stoichiometric cobaltates for both room and low temperatures. This is probably due to the repulsion of a randomly distributed Na atoms, locally violating hexagonal symmetry [18]. In the present investigation Na atoms are shifted back to their  $2d$  ideal sites. In order to avoid charge disproportionation which can arises from some Na distribution if the supercell is used in calculation, the change in the Na concentration has been considered in virtual crystal approximation (VCA) where each  $2d$  site is occupied by virtual atoms with fractional number of valence electrons  $x$  and a core charge  $10 - x$  instead of Na. Note, that all core states of virtual atom are left unchanged and corresponds to Na ones. We have chosen  $4s$ ,  $4p$ , and  $3d$  states of cobalt,  $2s$ ,  $2p$ , and  $3d$  states of oxygen, and  $3s$ ,  $3p$ , and  $3d$  states of Na as the valence states for TB-LMTO-ASA computation scheme [19]. The radii of atomic spheres were 1.99 au for Co, 1.61 au for oxygen, and 2.68 au for Na. Two classes of empty spheres (pseudo-atoms without core states) were added to fill the unit cell volume.

Crystal field of oxygen octahedron splits Co  $d$ -band into doubly degenerate  $e_g$  and triply degenerate  $t_{2g}$  subbands (without taking spin into account). LDA calculations show that those manifolds are separated by about 2 eV [4]. Here partially filled  $t_{2g}$  subband crosses the Fermi level whereas  $e_g$  subband due to strongly hybridization with nearest oxygen atoms is positioned well above the Fermi level. The procedure proposed in [20] allows one to calculate the Coulomb repulsion parameter  $U$  taking into account the screening of localized  $d$ -shell by itinerant  $s$ - and  $p$ -electrons. Resulting  $U$  is equal to 6.7 eV. However, the presence of the  $t_{2g}-e_g$  splitting give the reason to take into account an additional screening channel provided by the less localized  $e_g$  electrons. The value of  $U = 2.67$  eV for  $t_{2g}$  orbitals was calculated using the “constrained LDA” method [21], where the screening by the  $e_g$  electrons is also taken into account. This value was used in the present calculation for all doping concentrations  $x$ . Hund’s exchange parameter  $J$  depends weakly on screening effects due to its “on-site” character. Its value was also calculated within the “constrained LDA” method and was found to be 1.07 eV.

First, we have verified the possibility of HS state formation on Co  $d$ -shell. For this purpose the unit cell of  $\text{Na}_{0.61}\text{CoO}_2$  with two Co atoms was considered. We have started from a saturated A-type antiferromagnetic configuration with five electrons on the  $t_{2g}$  and one on the  $e_g$  shells. Small  $U = 2.67$  eV does not stabilize such magnetic configuration and LS state was obtained. Increasing  $U$  up to 5 eV however results in HS state with large local magnetic moment about  $1.96\mu_B$ . Nevertheless, this HS state has the total energy about 1.75 eV higher than the energy of a LS state. This large difference in total energy of both considered spin states arises from the hexagonal structure of cobaltates where the angle of Co–O–Co bond is close to  $90^\circ$  in contrast to almost  $180^\circ$  in, e.g.,  $\text{RCO}_3$  ( $\text{R} = \text{La}, \text{Ho}$ ). In the latter case the  $e_g$  band has the width of about 3–5 eV and its bottom lies just above the Fermi level. The system wins energy of  $2J$  forming a HS state overcoming the gap energy which is less than 1 eV. Due to this fact the difference between the LS and intermediate spin states in  $\text{RCO}_3$  is less than 250 meV [22]. The angle of Co–O–Co bond is close to  $90^\circ$  in cobaltates and it results in a weak overlap between  $e_g$  orbitals and hence in a narrow  $e_g$  band with larger gap between it and the  $t_{2g}$  band. Our calculation confirms that formation of the HS state in  $\text{Na}_x\text{CoO}_2$  is rather improbable and cannot be stabilized by any distortion of crystal structure or clusterization proposed in [17]. Local magnetic moments on Co sites can arise only because of the doped holes due to Na atoms deficiency. Those holes order on Co atoms and form nonmagnetic  $\text{Co}^{3+}$  and magnetic  $\text{Co}^{4+}$  ions with  $d^6$  and  $d^5$  configurations, respectively. In the following, we consider only the LS state.

The ordering of holes on  $t_{2g}$  shell and corresponding long-range magnetic and charge orders in  $\text{Na}_{0.5}\text{CoO}_2$  arise probably due to specific arrangement of Na atoms. These arrangements were observed experimentally [23] for several doping concentrations including  $x = 0.5$ . Proper description of such order within the “unrestricted Hartree–Fock” gives strong spin and orbital polarization and local magnetic moment of about  $1\mu_B$  on  $\text{Co}^{4+}$  sites as well as the insulating ground state with a sizable gap. To describe the non-ordered systems, the implementation of the “restricted Hartree–Fock” method is more suitable. In the latter, starting from the non-magnetic configuration of the  $d$ -shell with the equal number of spin-up and spin-down electrons, LDA+ $U$  method gives the non-magnetic solution without spin or orbital polarization. Note, that the gap does not open and  $\text{Na}_x\text{CoO}_2$  remains metallic for all Na concentration.

Obtained band structure of  $\text{Na}_x\text{CoO}_2$  for  $x = 0.33$ , 0.48, 0.61, and 0.72 are shown in Fig. 1. Dashed (black) lines correspond to LDA results whereas solid (red) lines are the bands obtained by LDA+ $U$  method. Cobalt  $d$  and oxygen  $p$  states are separated by a small

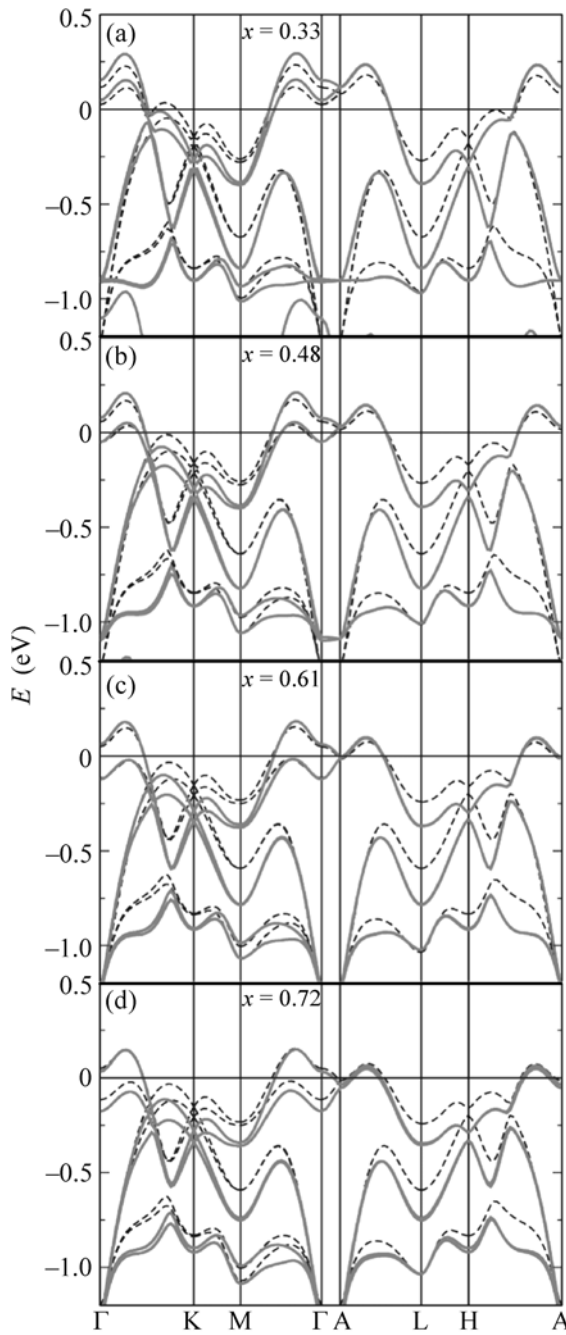


**Fig. 1.** Band structure of  $\text{Na}_x\text{CoO}_2$  for  $x$  equal to 0.33 (a), 0.48 (b), 0.61 (c), and 0.72 (d), obtained within LDA is shown by the black (dashed) curves. Band structures for the same doping concentrations within LDA+ $U$  are shown by the red (solid) curves.

gap of about  $-1.25$  eV for  $x = 0.61$  and  $x = 0.72$ . However, this gap disappears for lower doping concentration since the  $d$  band goes down when the number of  $d$  electrons decreases. The presence of the two  $\text{CoO}_2$  layers within the unit cell due to alternation of the oxygen arrangement results in a bonding–antibonding (bilayer) splitting, also present in Fig. 1.

The degeneracy of the  $t_{2g}$  levels is partially lifted by the trigonal crystal field distortion which splits them into the higher lying  $a_{1g}$  singlet and the two lower lying  $e_g'$  states. However, slight difference in occupation numbers of  $a_{1g}$  and  $e_g'$  orbitals (0.714 and 0.886, respectively, for  $x = 0.33$ ) results in a significant difference between the LDA+ $U$  and LDA band structures. The energy of the less occupied  $a_{1g}$  orbital increases for both spins, whereas all  $e_g'$  bands go down (the total  $a_{1g} - e_g'$  splitting becomes 0.21 eV for  $x = 0.33$ ). This makes six  $e_g'$  Fermi surface hole pockets to disappear for small  $x$  values. Note that for all Na concentration LDA+ $U$  predicts large  $a_{1g}$  Fermi pocket centered around the  $\Gamma$  point in excellent agreement with the ARPES spectra for  $x < 0.7$ . The additional electron pocket close to the  $\Gamma$  point appears in both LDA and LDA+ $U$  methods for a large doping concentrations. It was discussed in our previous work [24, 25] in connection with the electronic theory for the itinerant magnetism of highly doped compounds.

### 3. GUTZWILLER APPROXIMATION

For the small doping concentrations,  $x \approx 0.3$ , sodium cobaltate displays a canonical Fermi-liquid behavior both in resistivity [26] and in NMR relaxation rate [27]. Transport measurements [28] on single crystals with  $x = 0.7$  also revealed Fermi-liquid behavior at low temperatures. However, this behavior is characterized by the enormous electron-electron scattering. The Gutzwiller approximation [29–31] for the Hubbard model recommended itself as a good tool to describe low-energy quantities such as the FS and a ground state energy in the correlated metallic system. We will use the multiband generalization of this approximation [32] to investigate the effect of correlations on the bilayer splitting and compare it with the LDA+ $U$  results.

The Hamiltonian for  $\text{CoO}_2$ -plane in a hole representation is given by:

$$H = - \sum_{\mathbf{f}, \alpha, \sigma} \varepsilon^{\alpha} n_{\mathbf{f}\alpha\sigma} - \sum_{\mathbf{f}\mathbf{g}, \alpha, \beta, \sigma} t_{\mathbf{f}\mathbf{g}}^{\alpha\beta} d_{\mathbf{f}\alpha\sigma}^{\dagger} d_{\mathbf{g}\beta\sigma} + \sum_{\mathbf{f}, \alpha} U_{\alpha} n_{\mathbf{f}\alpha\uparrow} n_{\mathbf{f}\alpha\downarrow}, \quad (1)$$

where  $d_{\mathbf{f}\alpha\sigma}$  ( $d_{\mathbf{f}\alpha\sigma}^{\dagger}$ ) is the annihilation (creation) operator for the  $t_{2g}$  hole at Co site  $\mathbf{f}$ , spin  $\sigma$  and orbital index  $\alpha$ ,  $n_{\mathbf{f}\alpha\sigma} = d_{\mathbf{f}\alpha\sigma}^{\dagger} d_{\mathbf{f}\alpha\sigma}$ , and  $t_{\mathbf{f}\mathbf{g}}^{\alpha\beta}$  is the hopping matrix element between two lattice sites connected by the spatial vector  $(\mathbf{f} - \mathbf{g})$ ,  $\varepsilon^{\alpha}$  is the single-electron energies in which the chemical potential  $\mu$  is included. Since LDA-calculated hoppings and single-electron ener-

gies do not depend much on doping concentration [24, 25], we use here parameters for  $\text{Na}_{0.33}\text{CoO}_2$  from Table 1 of [25]. To take the bilayer splitting into account, we also consider hoppings  $t_z^{\alpha\beta}$  between the adjacent  $\text{CoO}_2$  planes. Their values were also derived from LDA results and are equal to  $t_z^{a_{lg}a_{lg}} = -0.0121$  eV,  $t_z^{e_g' e_g'} = 0.0080$  eV, and  $t_z^{e_g' e_g'} = -0.0086$  eV.

Within the Gutzwiller approximation the Hamiltonian describing the interacting system far from the metal-insulator transition for  $U \gg W$ ,  $J = 0$ , is replaced by the effective non-interacting Hamiltonian:

$$\begin{aligned} H_{\text{eff}} = & - \sum_{\mathbf{f}, \alpha, \sigma} (\varepsilon^\alpha + \delta\varepsilon^{\alpha\sigma} - \mu) n_{\mathbf{f}\alpha\sigma} \\ & - \sum_{\mathbf{f} \neq \mathbf{g}, \sigma} \sum_{\alpha, \beta} \tilde{t}_{\mathbf{f}\mathbf{g}}^{\alpha\beta} d_{\mathbf{f}\alpha\sigma}^\dagger d_{\mathbf{g}\beta\sigma} + \sum_{\alpha, \sigma} \delta\varepsilon^{\alpha\sigma} n_{\alpha\sigma}. \end{aligned} \quad (2)$$

Here,  $\tilde{t}_{\mathbf{f}\mathbf{g}}^{\alpha\beta} = t_{\mathbf{f}\mathbf{g}}^{\alpha\beta} \sqrt{q_{\alpha\sigma}} \sqrt{q_{\beta\sigma}}$  is the renormalized hopping,  $q_{\alpha\sigma} = \frac{x}{1 - n_{\alpha\sigma}}$ ,  $n_{\alpha\sigma} = \langle n_{\mathbf{f}\alpha\sigma} \rangle_0$  is the orbital filling factors,  $x = 1 - \sum_{\alpha\sigma} n_{\alpha\sigma}$  is the equation for the chemical potential.  $\delta\varepsilon^{\alpha\sigma}$  are the Lagrange multipliers yielding the correlation induced shifts of the single-electron energies. They are determined by minimizing the energy  $\langle H_{\text{eff}} \rangle_0$  with respect to the orbital filling factors  $n_{\alpha\sigma}$ . It is this energy shift  $\delta\varepsilon^{\alpha\sigma}$ , that forces the  $e_g'$  bands to sink below the Fermi level [33]. This is clearly seen in the doping-dependent evolution of the quasiparticle dispersion within the Gutzwiller approximation in Fig. 2. To obtain these figures we self-consistently solved equations on  $\delta\varepsilon^{\alpha\sigma}$  and on the chemical potential  $\mu$ .

The comparison of the Gutzwiller approximation results with the LDA+ $U$  dispersion reveals few very interesting conclusions. First, both approximations result in a suppression of  $e_g'$  hole pockets of the FS. Second, the bilayer splitting is strongly doping dependent and significantly reduced for the Gutzwiller quasiparticles in comparison with the LDA+ $U$  quasiparticles because the renormalization coefficient,  $\sqrt{q_{\alpha\sigma}} \sqrt{q_{\beta\sigma}}$ , occurs not only for the in-plane hoppings, but also for the inter-layer hoppings  $t_z^{\alpha\beta}$ . Third, when both bonding and antibonding  $t_{2g}$  bands do not cross the Fermi level around the  $\Gamma$  point, the FS crossings are the same in both approximations (see Fig. 2a). It is a simple consequence of the Luttinger theorem which holds for both approaches. But for large  $x$  due to the larger bilayer splitting in the LDA+ $U$  approach, the Fermi surfaces become different, while the Luttinger

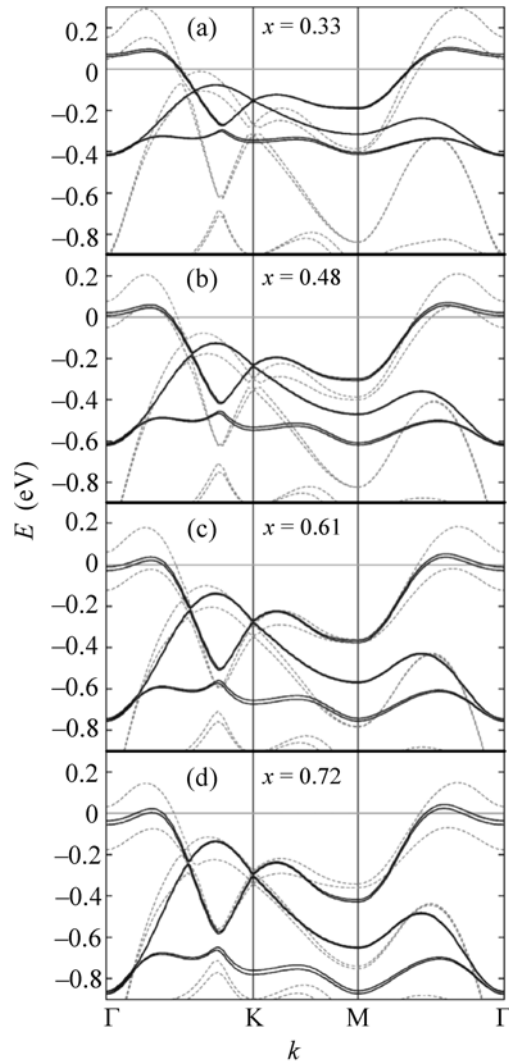


**Fig. 2.** Band structure of  $\text{Na}_x\text{CoO}_2$  for  $x$  equal to 0.33 (a), 0.48 (b), 0.61 (c), and 0.72 (d), obtained in LDA+ $U$  is shown by the dashed (red) curves. Dispersion within the Gutzwiller approximation is shown by the solid (black) curves.

theorem is again preserved. With an increase in the doping concentration  $x$ , the bandwidth of the Gutzwiller quasiparticles becomes closer to the LDA+ $U$  because the band renormalization factor  $\sqrt{q_{\alpha\sigma}} \sqrt{q_{\beta\sigma}}$  comes closer to unity.

Now we will discuss the correlations between our results and a more rigorous theory, namely, the Dynamical Mean Field Theory (DMFT). Generally, within DMFT the band structure of a Hubbard model consist of three parts: two incoherent Hubbard subbands and a coherent near-Fermi-level quasiparticle band. Since  $U$  is not very large in sodium cobaltates, Hubbard subbands lose their spectral weight and are almost merged with the coherent band. Thus, low-energy excitations are determined mostly by this qua-

siparticle band. And it is this band that revealed within the Gutzwiller approximation, even if we formally in the limit of  $U \gg W$ .

In the case of  $\text{Na}_x\text{CoO}_2$ , DMFT calculations show that for the small  $U$  and a non-zero  $J$ ,  $e_g'$  FS pockets can be stabilized [34, 35]. On the other hand, more recent DMFT calculations of [36] confirm results of the Gutzwiller approximation provided that the crystal field splitting  $\Delta$  is about 50 meV. This value is in agreement with our value of  $\Delta = 53$  meV [25], so our results are consistent with DMFT.

#### 4. CONCLUSIONS

In the present work employing ab-initio “constrained LDA” method we obtained Coulomb repulsion parameter  $U = 2.67$  eV for  $t_{2g}$  orbitals taking into account the screening by the  $e_g$ -electrons in addition to the screening by the itinerant  $s$ - and  $p$ -electrons. Hund’s exchange parameter was found to be  $J = 1.07$  eV.

Also we have shown that due to the Co–O–Co bond angle being close to  $90^\circ$  in  $\text{Na}_x\text{CoO}_2$ , the energy gap between the LS and HS states is too large to be overcome by the clusterization or reasonable distortions of the crystal structure. Thus we conclude that realization of the HS state is highly improbable in these particular substance.

To analyze the effect of electronic correlations on the Fermi surface topology of  $\text{Na}_x\text{CoO}_2$  we use two approaches, non-magnetic LDA+ $U$  and the Gutzwiller approximation for the Hubbard-type model based on the LDA band structure. Physically, the reason of  $e_g'$  FS pockets disappearance is quite clear. Within LDA+ $U$  the energy of the less occupied  $a_{1g}$  orbital increases for both spins, whereas all  $e_g'$  bands go down. This makes six  $e_g'$  FS hole pockets to disappear for small  $x$  values, in agreement with ARPES for  $x < 0.7$ . Gutzwiller approximation also resulted in a suppression of  $e_g'$  hole pockets at the FS. Most importantly, the bilayer splitting was found to be strongly doping dependent and significantly reduced for the Gutzwiller quasiparticles in comparison with the LDA+ $U$  quasiparticles. This may explain why the bilayer splitting is not observed in ARPES though it is very pronounced in the LDA band structure.

The authors thank I. Eremin, M. Laad, and S.G. Ovchinnikov for useful discussions. A.S. and V.I.A. acknowledge the support of the Russian Foundation for Basic Research (project nos. 10-02-00046-a, 09-02-00431-a, and 10-02-00546-a), the Council of the President of the Russian Federation for Support of Young Scientists and Leading Scientific Schools (project nos. NSh-1941.2008.2 and MK-3758.2010.2), the Presidium of the Russian Academy

of Science (programs “Quantum Microphysics of Condensed Matter” N7 and “Strongly Compressed Materials”), and the Russian Federal Agency for Science and Innovations (project no. 02.740.11.0217). M.M.K. acknowledges the support of INTAS (YS Grant no. 05-109-4891); the Russian Foundation for Basic Research (project nos. 09-02-00127, 06-02-16100, and 06-02-90537-BNTS); the Siberian Branch, Russian Academy of Sciences (integration program no. 40); the Presidium of the Russian Academy of Sciences (program no. 5.7); the Council of the President of the Russian Federation for Support of Young Scientists and Leading Scientific Schools (project no. MK-1683.2010.2); and the Ministry of Education and Science of the Russian Federation (project no. R891, federal program “Scientific and Pedagogical Personnel of Innovative Russia for 2009–2013”).

#### REFERENCES

1. N. B. Ivanova, S. G. Ovchinnikov, and M. M. Korshunov, *Phys. Usp.* **52**, 789 (2009).
2. K. Fujita, T. Mochida, and K. Nakamura, *Jpn. J. Appl. Phys.* **40**, 4644 (2001).
3. K. Takada, H. Sakurai, E. Takayama-Muromachi, et al., *Nature (London)* **422**, 53 (2003).
4. D. J. Singh, *Phys. Rev. B* **61**, 13397 (2000).
5. K.-W. Lee, J. Kuneš, and W. E. Pickett, *Phys. Rev. B* **70**, 045104 (2004).
6. M. Z. Hasan, Y.-D. Chuang, D. Qian, et al., *Phys. Rev. Lett.* **92**, 246402 (2004).
7. H.-B. Yang, S.-C. Wang, A. K. P. Sekharan, et al., *Phys. Rev. Lett.* **92**, 246403 (2004).
8. H.-B. Yang, Z.-H. Pan, A. K. P. Sekharan, et al., *Phys. Rev. Lett.* **95**, 146401 (2005).
9. D. Qian, L. Wray, D. Hsieh, et al., *Phys. Rev. Lett.* **96**, 046407 (2006).
10. D. Qian, D. Hsieh, L. Wray, et al., *Phys. Rev. Lett.* **96**, 216405 (2006).
11. Y. Wang, N. S. Rogado, R. J. Cava, and N. P. Ong, *Nature (London)* **423**, 425 (2003).
12. P. Zhang, W. Luo, M. L. Cohen, and S. G. Louie, *Phys. Rev. Lett.* **93**, 236402 (2005).
13. L.-J. Zou, J.-L. Wang, and Z. Zeng, *Phys. Rev. B* **69**, 132505 (2004).
14. V. I. Anisimov and O. Gunnarsson, *Phys. Rev. B* **43**, 7570 (1991).
15. I. Yang, S. Y. Savrasov, and G. Kotliar, *Phys. Rev. Lett.* **87**, 216405 (2001).
16. A. G. Petukhov, I. I. Mazin, L. Chioncel, and A. I. Lichtenstein, *Phys. Rev. B* **67**, 153106 (2003).
17. M. Daghofer, P. Horsch, and G. Khaliullin, *Phys. Rev. Lett.* **96**, 216404 (2006).
18. J. D. Jorgensen, M. Avdeev, D. G. Hinks, et al., *Phys. Rev. B* **68**, 2145171, (2003).
19. O. K. Andersen and O. Jepsen, *Phys. Rev. Lett.* **53**, 2571 (1984).

20. O. Gunnarsson, O. K. Andersen, O. Jepsen, and J. Zaanen, Phys. Rev. B **39**, 1708 (1989).
21. W. E. Pickett, S. C. Erwin, and E. C. Ethridge, Phys. Rev. B **58**, 1201 (1998).
22. I. A. Nekrasov, S. V. Streltsov, M. A. Korotin, and V. I. Anisimov, Phys. Rev. B **68**, 235113 (2003).
23. H. W. Zandbergen, M. Foo, Q. Xu, et al., Phys. Rev. B **70**, 024101 (2004).
24. M. M. Korshunov, I. Eremin, A. Shorikov, and V. I. Anisimov, JETP Lett. **84**, 650 (2006).
25. M. M. Korshunov, I. Eremin, A. Shorikov, et al., Phys. Rev. B **75**, 094511 (2007).
26. M. L. Foo, Y. Wang, S. Watauchi, et al., Phys. Rev. Lett. **92**, 247001 (2004).
27. F. L. Ning, T. Imai, B. W. Statt, and F. C. Chou, Phys. Rev. Lett. **93**, 237201 (2004).
28. S. Y. Li, L. Taillefer, D. G. Hawthorn, et al., Phys. Rev. Lett. **93**, 056401 (2004).
29. M. C. Gutzwiller, Phys. Rev. Lett. **10**, 159 (1963); Phys. Rev. A **134**, 923 (1964); Phys. Rev. A **137**, 1726 (1965).
30. F. Gebhard, Phys. Rev. B **41**, 9452 (1990).
31. G. Kotliar and A. E. Ruckenstein, Phys. Rev. Lett. **57**, 1362 (1986).
32. J. Bünenmann, F. Gebhard, and W. Weber, J. Phys.: Cond. Mat. **9**, 7343 (1997).
33. S. Zhou, M. Gao, H. Ding, et al., Phys. Rev. Lett. **94**, 206401 (2005).
34. H. Ishida, M. D. Johannes, and A. Liebsch, Phys. Rev. Lett. **94**, 196401 (2005).
35. C. A. Perroni, H. Ishida, and A. Liebsch, Phys. Rev. B **75**, 045125 (2007).
36. C. A. Marianetti, K. Haule, and O. Parcollet, Phys. Rev. Lett. **99**, 246404 (2007).